VISUALIZATION OF TURBULENT THERMAL MIXING STRUCTURES IN A HORIZONTAL STRATIFIED CONDENSING FLOW

Seungtae Lee, Dong-Jin Euh, and Chul-Hwa Song*
Korea University of Science & Technology / Korea Atomic Energy Research Institute
Daedeok-Daero 989-111, Yuseong-Gu, Daejeon, Rep. of KOREA
leest@kaeri.re.kr; djeuh@kaeri.re.kr; chsong@kaeri.re.kr

ABSTRACT

The main objective of this study is to experimentally investigate the turbulent thermal mixing structures of a co-current steam-water stratified flow in a horizontal rectangular channel by visualizing the liquid motion, which causes a mixing and stratification of hot and cold-water by exchanging the mass, momentum, and energy at the gas-liquid interface. This work presents experimental measurements of the temperature and velocity distributions of the water layer in a co-current stratified two-phase flow for condensing steam-water cases at an atmospheric pressure condition. A PIV and LIF method was used to measure the velocity distribution and the temperature distribution of the water layer. Interfacial heat transfer coefficient and turbulent heat flux were evaluated from the measured velocity and temperature distributions. Based on the experimental data, the phenomenological analysis of turbulent thermal mixing structures in a co-current stream-water stratified flow have been proposed.

KEYWORDS
Direct-contact condensation, Horizontal stratified flow, Turbulent thermal mixing, Flow visualization

1. INTRODUCTION

The direct contact condensation occurring in a steam-water stratified flow is an important thermal-hydraulic phenomenon relevant to the safety of nuclear reactor systems. For a pressurized thermal shock (PTS) in a partially water-filled cold-leg, mixing of hot and cold-water, and the direct contact condensation (DCC) heat transfer in a horizontal flow zone can be frequently encountered in postulated accident situations. A condensation-induced water hammer (CIWH) in horizontal pipes, which initially occurs by DCC of steam on the subcooled water in a horizontal stratified flow, is another important engineering safety issue. The modeling of DCC in a steam-water stratified flow is particularly important in the analysis of PTS and CIWH.

A number of experimental studies [1-6] have been previously performed to investigate the DCC phenomena for a stratified two-phase flow in a horizontal flow channel. Empirical correlations for the DCC heat transfer were derived in the form of a power-law relationship of the parameters from the experimental measurements. However, most of the previous experimental studies have been adopted point-wise devices, such as thermocouples and pitot tubes, to measure the temperature and velocity profiles in a flow. Even though local measurements can provide information about the interfacial heat transfer characteristics, their usage is rather limited compared to the field-wise measurements. The intrusive characteristics are another

weakness that the previous point measurement data have. Moreover, the visualized experimental data for the flow motion and turbulence structure caused by DCC in a stratified flow are still insufficient. A precise observation for the turbulent thermal mixing and interfacial characteristics is required for the analysis of DCC heat transfer phenomenon in a horizontal stratified flow.

The objective of this study is to experimentally investigate the flow characteristics of co-current steam-water stratified flow in a horizontal rectangular channel by visualizing the liquid motion, which causes a mixing and stratification of hot and cold-water by exchanging the mass, momentum, and energy at the gas-liquid interface. The current work presents the temperature and velocity distributions of the water layer experimentally in a co-current stratified two-phase flow for condensing steam-water cases under atmospheric pressure condition. Based on the experimental data for a co-current stratified two-phase flow in condensing steam-water conditions, basic strategy of analysis method was proposed for the interface configuration and turbulent thermal mixing mechanisms.

2. EXPERIMENTS

In the present study, visualization experiments were carried out to investigate the turbulent characteristics of the water layer for steam-water stratified flows in a horizontal rectangular channel. The PIV method was used to measure the velocity distribution of the water layer. The LIF method was used to measure the temperature distribution of the water layer. The interfacial heat transfer coefficient and the turbulent heat flux were also evaluated from the measured velocity and temperature distributions.

2.1. Experimental Apparatus

Figure 1 shows a schematic of the Horizontal Condensing two-phase flow test loop (HOCO) used in the present study. The HOCO was designed and constructed in such a way that the DCC of steam in a stratified flow and the behavior of the water layer along the horizontal channel can be easily measured in a steam-water or air-water flow with either a co-current or counter-current flow configuration. The test loop consists of a test section; supply systems of air, steam, and water; a control system; and data acquisition system.

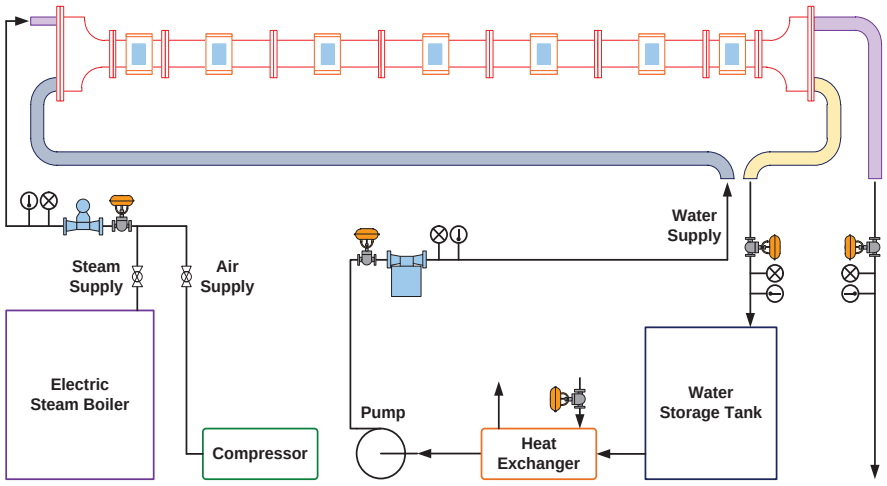

Figure 1. Schematic of the HOCO test loop

Steam is produced by an electric steam boiler with a maximum power of 100 kW, and air is supplied from a compressor. The water is pumped from a storage tank to the test section. The water temperature is controlled by adjusting the secondary flow of the heat exchanger located upstream of the pump. The rates of volumetric air and steam flow injected into the test section are measured independently by a vortex

flowmeter. The mass flow rate of the water injected into the test section is measured by a Coriolis flowmeter. The density of the air, steam, and water is estimated from the temperature and pressure measured by thermocouples and pressure transmitters, respectively.

Figure 2 shows a schematic of the test section. The test section has a rectangular cross-section with a length of 1.850 m, a width of 0.08 m, and a height of 0.06 m. The test section is made of stainless steel 10 mm thick. In order to visualize the stratified two-phase flow, Pyrex-glass windows (40 mm * 60 mm) are installed in the front and top of the channel, and polycarbonate windows (40 mm * 80 mm) are installed at the bottom of the channel. As shown in Fig. 2(c), these windows are located at 0.265, 0.595, 0.925, 1.255, and 1.585 m from the end of the inlet plate, which is installed for the separation of the injected water and gas flow.

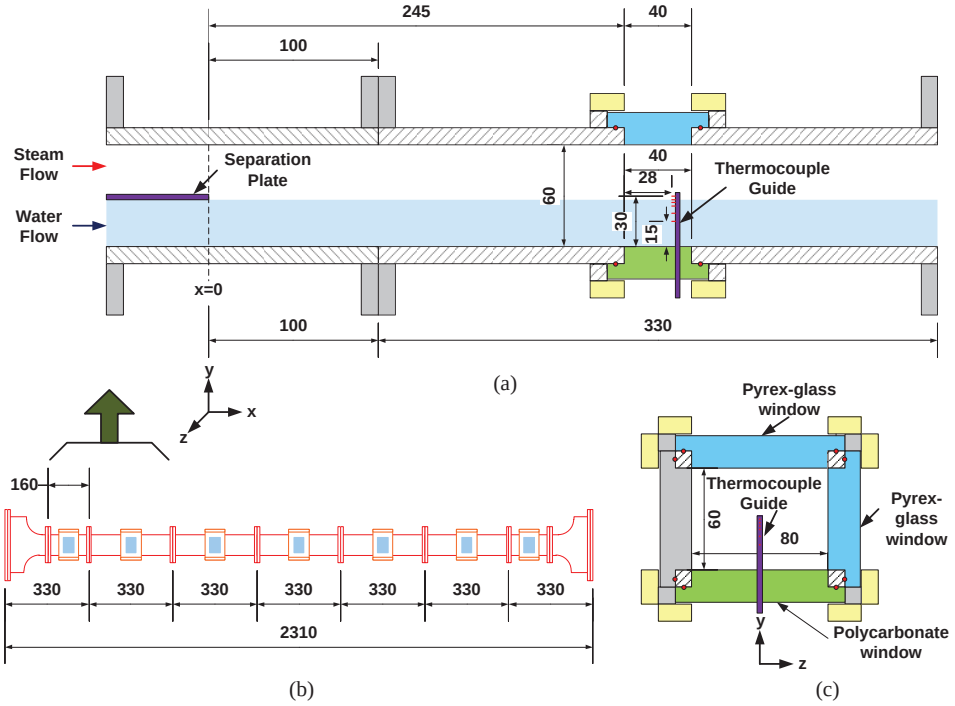

Figure 2. Schematic of the test section: (a) Inlet section and thermocouples installation, (b) Axial dimension of test section, (c) Cross-sectional view.

2.2. Simultaneous PIV/LIF measurements

In this study, a particle image velocimetry (PIV) technique and a laser induced fluorescence (LIF) technique are applied to the simultaneous measurement of the water layer velocity distributions and the water layer temperature distributions, respectively. A schematic arrangement of the optical setup for the simultaneous PIV/LIF measurement system is shown in Fig. 3 together with the ultrasonic measuring system. The PIV and LIF images are acquired simultaneously using two charge-coupled device (CCD) cameras. The PIV image is acquired by a Vision Research Phantom V711 CCD camera with a resolution of 960*800 and acquisition frequency of 500 Hz. The LIF image is acquired using Princeton Instruments Megaplus ES4040 CCD camera with a resolution of 1600*1600 and acquisition frequency of 10 Hz.

The cameras are installed perpendicularly, and the beam splitting optic is placed between the cameras and the sight glass of the test section at a 45 degree angle. The beam splitting optic splits the incident light into 50% transmitted light and 50% reflected light. The transmitted light is transferred to the PIV camera, and the reflected light is transferred to the LIF camera. A Litron Lasers LDY302 PIV pulsed Nd:YLF laser with

an emission wavelength of 527 nm and power of 20 mJ is adopted and synchronized with the camera using a pulse generator. A laser beam emitted from the pulsed Nd:YLF laser is expanded using a plano-concave cylindrical lens to form a planar laser sheet, and the thickness of the planar laser sheet is minimized in a water layer using a plano-convex cylindrical lens.

Silver-coated particles with a mean diameter of 10 micro meters are used for the PIV measurement, and Rhodamine-B temperature sensitive fluorescence dye is used for the LIF measurement. The particle and fluorescence dye are pre-mixed with de-ionized water in a water storage tank. The concentration of fluorescence dye in the water is carefully controlled at about 0.25mg/l. The light incident on the camera includes both illuminated particles and fluorescence through the use of a laser light sheet. A long pass filter with 560 nm is installed in front of the LIF camera to eliminate any incident particle light that may be illuminated.

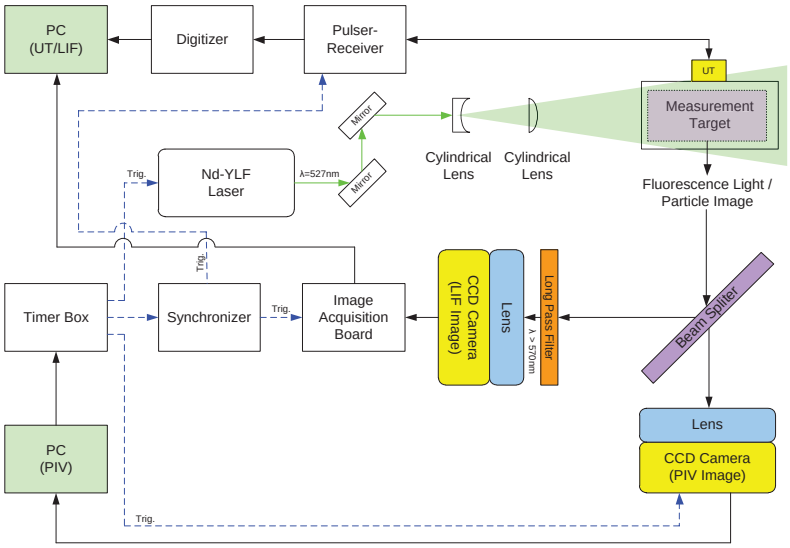

Figure 3. Schematic diagram of the simultaneous PIV/LIF/UT measurement systems.

2.3. Experimental Conditions

In this study, effects of non-condensable gas were not examined. The experiments were conducted by varying the steam flow rate to adjust the superficial velocity of steam phase. The present test conditions are summarized in Table 1. The superficial velocity of the inlet water is fixed at 0.025 m/s. The superficial velocity of the inlet steam is varied from 1.2 m/s to 2.8 m/s. The vertical location (y-direction) of the inlet plate bottom surface is fixed at 28 mm, and the water layer thickness at an axial location (x-direction) of 0.265 m is fixed at 28 mm. The system pressure is atmospheric pressure and the saturated steam is injected into the test section. The experimental results taken at an axial location of 0.265, 0.595 and 0.925 m downstream of the end of the inlet plate.

Table I. Test matrix of the present experiments

Experiments	$T_{f,in}$ (℃)	$T_{g,in}$ (℃)	$j_{f,in}$ (℃)	$j_{g,in}$(℃)	Number of data
Co-Current Steam-Water	28.5-32.0	99.5-100	0.0244-0.0250	1.19-2.82	9

2.4. Measurement Uncertainties

Uncertainties of the experimental parameters are estimated according to the International Organization for Standardization (ISO) Guide to the Expression of Uncertainty in Measurement (1995), or ISO GUM. The uncertainty analysis is performed in accordance with a 95% confidence level. The estimated overall uncertainty of each measurement parameter is summarized in Table 2.

Table II. Estimated uncertainty of the individual measurement parameters

Parameter	Overall uncertainty
Inlet water flow rate (%)	**2.1**
Inlet gas flow rate (%)	**1.3**
Inlet flow temperature (°C)	**1.0**
Local water layer velocity (%)	**2.7**
Local water layer temperature (°C)	**3.2**

3. EXPERIMENTAL RESULTS

3.1. Water Temperature and Velocity

Figure 4 shows the vertical profiles of the mean values of temperature in a water layer at two different axial locations of the channel for various superficial steam velocities. The temperature in a water layer increases as approaching closer to the phasic interface. When the superficial steam velocity is 1.2 m/s, it can be observed that the temperature variation and its gradient in a water layer close to the bottom surface (i.e., y/δ_f<0.6 at x=0.602 m, y/δ_f<0.7 at x=0.932 m) is fairly small. While flowing downstream, the length of the uniform temperature region is decreased due to an accumulation of condensate and thermal mixing. With an increase the steam velocity, the water layer temperature of the lower region does not remain constant, but rises more or less gradually. The temperature gradient in a water layer in the lower region indicates the thermal mixing between the condensate and the injected cold-water.

Figure 5 ~ 7 show the mean vertical profiles of the streamwise velocity (u) in a water layer for various superficial gas velocities at the three axial locations of the channel (x=0.265, 0.595, and 0.925 m). The mean streamwise velocity ($\bar{u}$) and the vertical distance (y) are normalized by the mean inlet water velocity ($\overline{V_{in}}$) and the mean water layer thickness ($\overline{\delta_f}$) respectively.
The water layer can be divided into three zones in the vertical direction: (1) the region close to the bottom solid wall (wall region), (2) the interfacial region influenced by the interfacial dynamics (interfacial region), and (3) the intermediate region between the wall region and the interface region (buffer region). The velocity of the water layer is increased with the steam flow in the interfacial region (i.e., y/δ_f>0.6 for j_g=1.2 m/s and y/δ_f>0.4 for j_g=2.0 m/s at x=0.265 m). When increasing the steam velocity and flowing downstream, the length of the buffer region is decreased. In addition, the streamwise velocity in the buffer region and the wall region (y/δ_f<0.7 at x=0.595 m) decreases when the steam velocity increases.

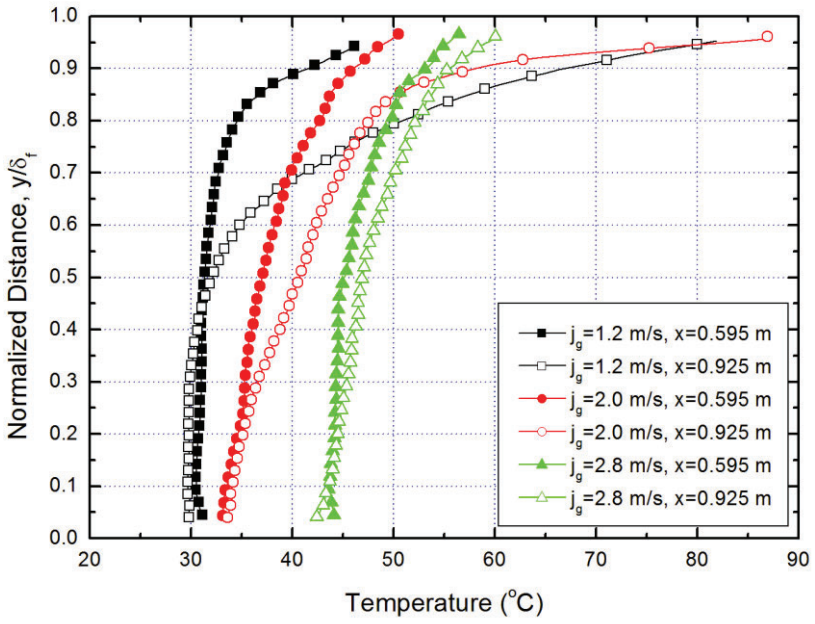

Figure 4. Mean vertical profiles of temperature in a water layer

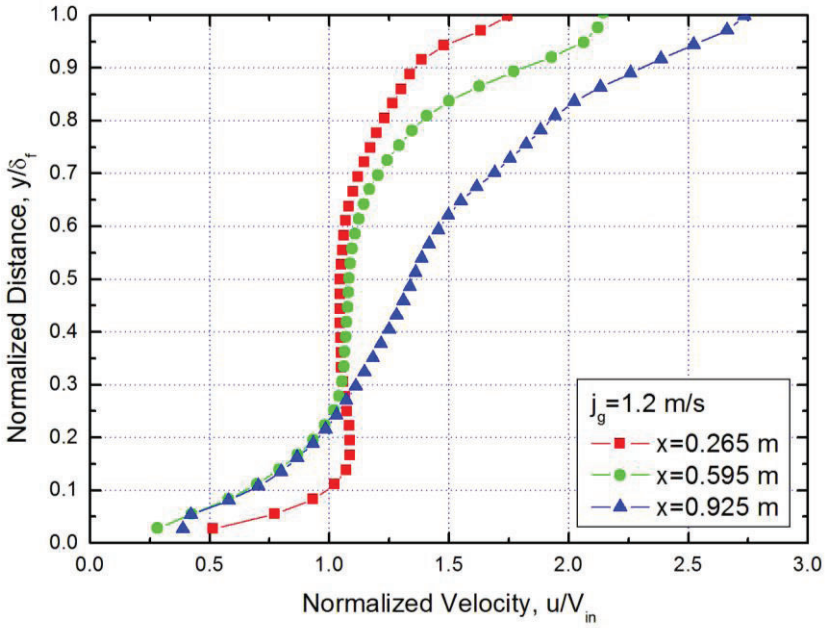

Figure 5. Mean vertical profiles of streamwise velocity in a water layer (j_g=1.2 m/s)

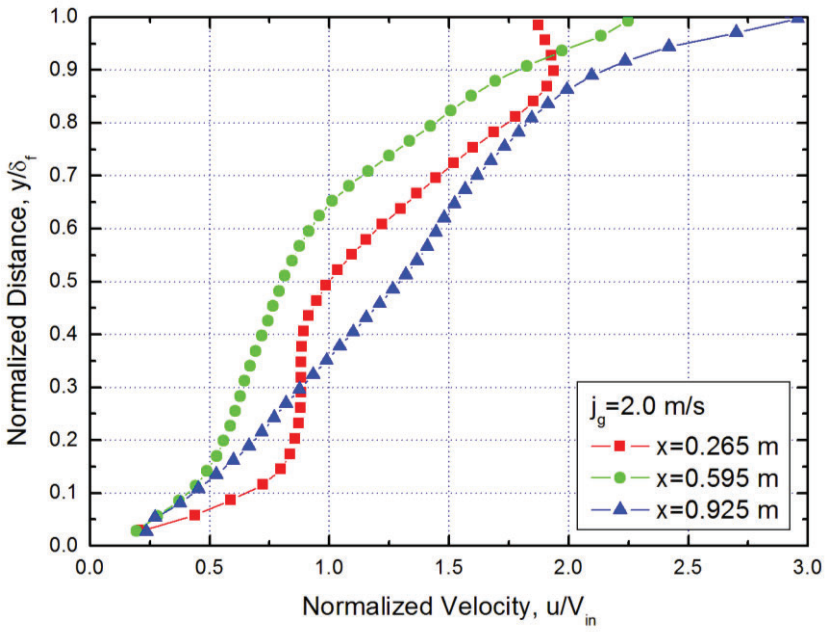

Figure 6. Mean vertical profiles of streamwise velocity in a water layer (j_g=2.0 m/s)

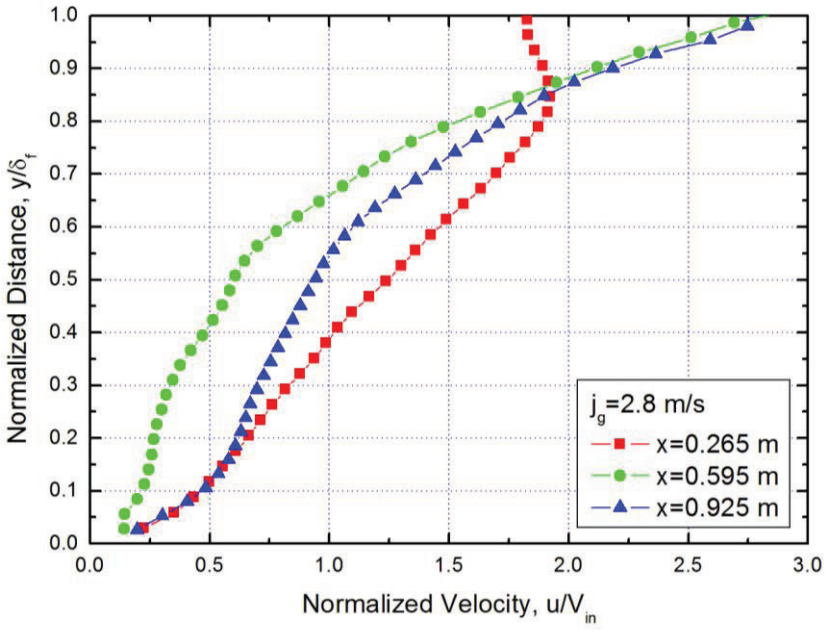

Figure 7. Mean vertical profiles of streamwise velocity in a water layer (j_g=2.8 m/s)

3.2. Local Liquid Nusselt Number

The interfacial heat transfer coefficient been evaluated from the measurement of increasing rate of water bulk temperature owing to steam condensation. The measured velocity and temperature profiles of the water layer and the water layer thickness were used to evaluate the water bulk temperature increasing rate along the axial direction.

Local mass flow rate of the water can be expressed from the relations of the mass and energy conservation for a control volume. Local mass flow rate of the water is evaluated from the increase of the water layer enthalpy ($i_f = C_{pf}T_f$) as follows:

$$W_f(x) = \frac{W_f(0)\left[C_{pf}T_f(0) - i_g\right]}{C_{pf}T_f(x) - i_g} \tag{1}$$

Local mass flow rate of the water is function of local bulk water temperature, so local mass flow rate of the water can be evaluated from the local water bulk temperature. The water bulk temperature (T_f) at any axial location is evaluated by integrating the measured local water layer temperature and velocity over the area of the water layer divided into thin rectangular cells with a height (y) of 0.1 mm as follows:

$$T_f(x) = \frac{\int \rho_f(x,y,z)T_f(x,y,z)V_f(x,y,z)dydz}{\int \rho_f(x,y,z)V_f(x,y,z)dydz} \tag{2}$$

The local interfacial heat transfer coefficient is estimated by using the gradient of the local flow rate of the water. Based on the mass and energy balance, the local interfacial heat transfer coefficient at x can be expressed as follows:

$$h(x) = \frac{i_{fg}}{S_i\left[T_g - T_f(x)\right]}\frac{dW_f}{dx} \tag{3}$$

The average heat transfer coefficient can be obtained by integrating the local interfacial heat transfer coefficient over the axial length of interface.

$$\begin{aligned}\bar{h} &= \frac{1}{x}\int_0^x h(x)dx \\ &= \frac{C_{pf}}{xS_i}\left(\left\langle W_f(0)\left\{\frac{C_{pf}\left[T_g - T_f(0)\right]}{i_{fg}} + 1\right\}\right\rangle ln\left\langle\frac{W_f(0)C_{pf}\left[T_g - T_f(0)\right]}{W_f(0)\left\{C_{pf}\left[T_g - T_f(0)\right] + i_{fg}\right\} - W_f(x)i_{fg}}\right\rangle - W_f(x) + W_f(0)\right)\end{aligned} \tag{4}$$

The definitions of dimensionless numbers used in the present study are as follows:

$$\begin{gathered} Nu = \frac{\boldsymbol{h}D_{h,f}}{k_f} \\ \boldsymbol{Re_g} = \frac{\rho_g u_g D_{h,g}}{\mu_g}\,,\ \boldsymbol{Re_f} = \frac{\rho_f u_f D_{h,f}}{\mu_f} \\ \boldsymbol{D_{h,g}} = \frac{4A_{c,g}}{S_i + S_g}\ ,\ \boldsymbol{D_{h,f}} = \frac{4A_{c,f}}{S_i + S_f} \end{gathered} \tag{5}$$

Figure 8 shows the increase of the interfacial heat transfer coefficient as a function of inlet superficial steam velocity at the two axial locations of the channel (x=0.602, 0.932 m). The interfacial heat transfer coefficient increases clearly with an increase in the steam flow rate. The estimated heat transfer coefficient is analyzed with a maximum error of 9.5%.

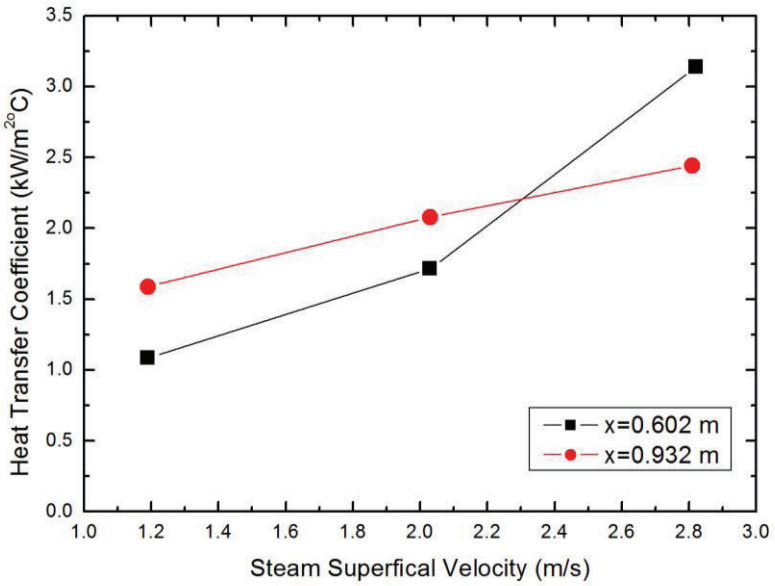

Figure 8. Average interfacial heat transfer coefficient

Figure 9 shows the comparison of the Nusselt numbers estimated from the experimental data with calculated from existing correlations. Kim et al.'s [3] correlation with the Froude number and Lim et al.'s [2] correlation for wavy flow underestimate the experimental Nusselt numbers. Both correlations were obtained from the rectangular channel experimental data. Although the Kim et al.'s correlation was obtained from the counter-current flow experiment data, shows the better accurate prediction. Lim et al.'s correlation significantly under estimated the interfacial heat transfer, probably because the water layer thickness did not take into account in this correlation. The results show that the liquid layer thickness is better correlating parameter for the interfacial heat transfer coefficient.

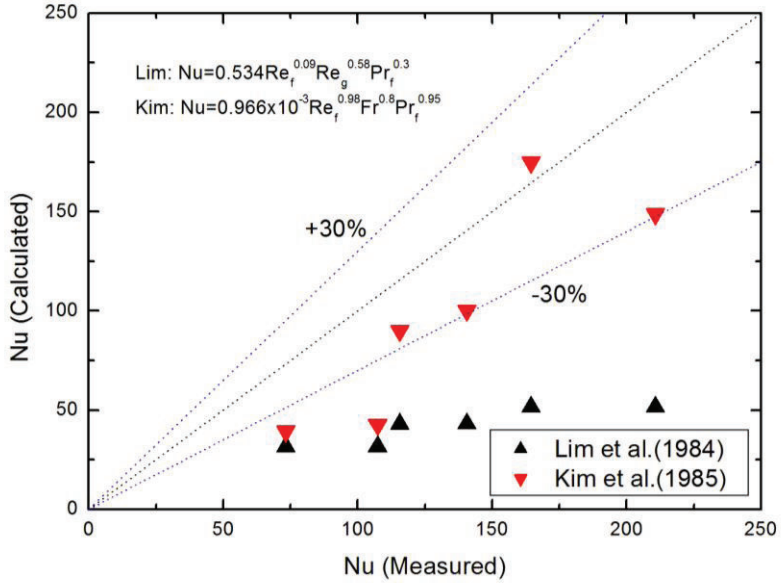

Figure 9. Comparison of the present Nusselt numbers with Lim's and Kim's correlation

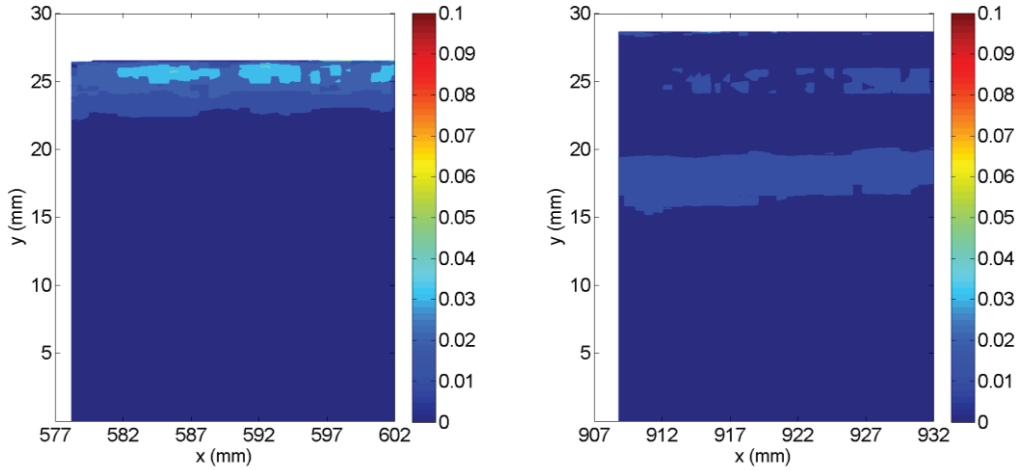

(a) x=0.577~0.602 m, j_g=1.2 m/s (b) x=0.907~0.932 m, j_g=1.2 m/s

(c) x=0.577~0.602 m, j_g=2.0 m/s (d) x=0.907~0.932 m, j_g=2.0 m/s

(e) x=0.577~0.602 m, j_g=2.8 m/s (f) x=0.907~0.932 m, j_g=2.8 m/s

Figure 10. Mean turbulent heat flux fields in a water layer

3.3. Turbulent Heat Flux

Figure 10 show the mean value of 100 instantaneous turbulent heat flux ($T'v'$) distribution in the water layer for various superficial steam velocities at the two axial locations of the channel. The turbulent heat flux is calculated as follows:

$$\overline{v_i' T_i'} = \frac{1}{N} \sum_{i=1}^{N} v_i' T_i' \tag{6}$$

where the temperature fluctuations (T') and vertical velocity fluctuations are calculated as follows:

$$T_i' = T_i - \bar{T} \, , \, v_i' = v_i - \bar{v} \tag{7}$$

where the ensemble-average temperature ($\bar{T}$) of the instantaneous temperature (T_i) and average velocity component ($\bar{v}$)of the instantaneous velocity component (v_i) are calculated as follows:

$$\bar{T} = \frac{1}{N} \sum_{i=1}^{N} T_i \, , \, \bar{v} = \frac{1}{N} \sum_{i=1}^{N} v_i \tag{8}$$

Figure 11 compare the profiles of the turbulent heat flux in a water layer for various superficial steam velocities at the two axial locations of the channel (x=0.595 and 0.925 m). The turbulent heat flux are increased with the increase of steam flow rate in steam-water flow conditions. In the case of x=0.595 m and j_g=1.2 m/s, at around y/δ_f>0.6, the mean turbulent heat flux of the water layer tend to increase markedly. In the case of j_g=1.2 and 2.0 m/s, the turbulent heat flux increases in the whole region of the water layer. The condensate that propagated into the water layer have strong effect on temperature and vertical velocity component fluctuations. The increased turbulent heat flux indicates the turbulent thermal mixing between the condensate and the injected cold-water. While going downstream, the results of the decreased turbulent thermal mixing between the condensate and the injected cold-water, turbulent heat flux are decreased.

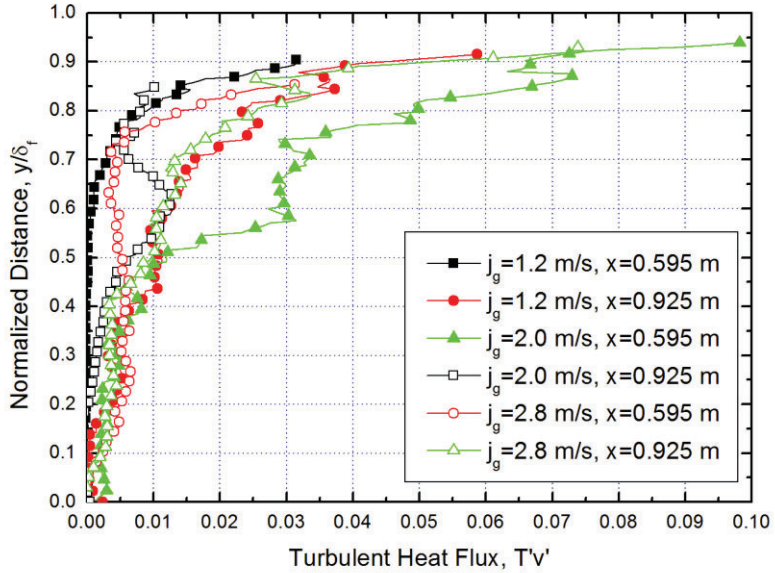

Figure 11. Mean vertical profiles of turbulent heat flux in a water layer (x=0.595 m)

3.4. Turbulent Mixing Mechanism

In the gas-water horizontal stratified flow, gas phase and liquid phase form a phasic interface. The lighter gas fluid is located on the upper part of heavier liquid fluid. In the steam-water horizontal stratified flow, an additional interface can be considered in liquid layer. The condensed higher temperature low density water is located on top of the lower temperature high density water. If a lighter fluid is located on the upper part of heavier liquid fluid, the flow is statically stable because of the restriction of vertical motions induced by a buoyancy force. However, in some cases, a velocity shear destabilizes a vertical stratification. The kinetic energy supplied by the flow is converted into the potential energy and in some cases increased potential energy overcome buoyancy force. This instability causes water to move vertically and results in mixing.

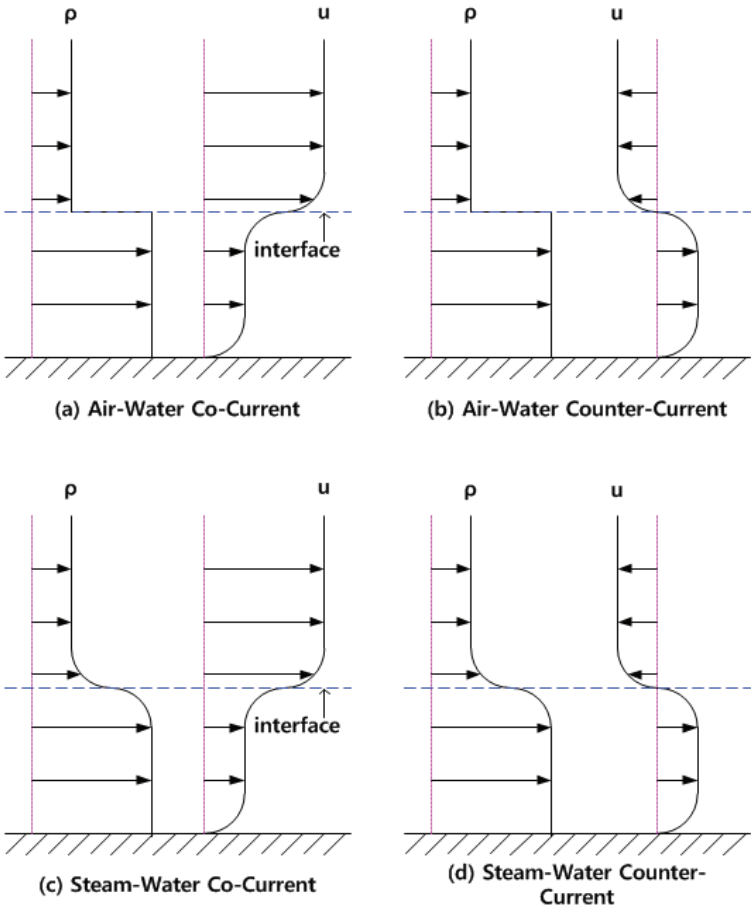

Figure 12. Schematic density and streamwise velocity profiles in a horizontal stratified

Figure 12 illustrates the density and the streamwise velocity distributions in various conditions of gas-liquid horizontal stratified flow. Depending on the velocity gradient, the water layer can be divided into two layers and an interface between the two-layers are defined as an internal interface. The water layer flowing at different velocities are produced by an interfacial shear. When a shear is presented, the internal interfacial waves may grow and lead to generate the mixing between the two layers.

In the steam-water co-current flow conditions, the high temperature low density condensate are penetrating below of internal interface. The kinetic energy generated by the interfacial shear is converted to the potential energy. The internal interface continuously falls to the bottom region that increases in potential energy along

with the loss of the kinetic energy. The loss of the kinetic energy reduces shear in the water layer that velocity gradient will be flattened. If the potential energy is maximized, the flow is statistically unstable, and then the reordering of the buoyancy force decreases the potential energy meanwhile generating the kinetic energy. Finally the flow will be statistically stabilized. This energy exchange process leads a turbulent thermal mixing.

In the steam-water counter-current flow conditions, the low temperature high density water moves to above the internal interface. The potential energy will be increased near the internal interface, and then the increased potential energy will generate the turbulent thermal mixing, as in the steam-water co-current flow conditions. However, the decreased kinetic energy will be recovered by the decrease in potential energy. This means that turbulent thermal mixing will not propagate to the bottom region. It is restricted at around the internal interface, as already pointed out by earlier researchers [4-6]. With the increase in the interfacial shear, the liquid velocity at steam-water interfaces becomes negative. In this condition, the high temperature low density water penetrates to the bottom direction, and the low temperature high density water rises. In this condition, flow will exhibit more large scale turbulent motion.

This different flow mixing phenomena leads to a relatively larger interfacial heat transfer in the co-current flow than that in the counter-current flow at the same flow velocity conditions. The sign and magnitude of the velocity gradient depend on the relative velocity between the two fluid layers. As already pointed out by earlier researchers, the interfacial heat transfer increases with an increase in the steam and water flow rate [2-6]. However, they applied the effect of the steam and water flow rate on the heat transfer separately. Without considering the relative velocity between the two fluid layers, they observed discrepancy between the measured and the empirically correlated condensation rate [4-6].

The vertical liquid motions that transport the thermal energy away from the steam-water interface can increase the steam condensation rate. With an increase in the vertical mixing depth, the volume of bulk water mixed with the condensate will be increased since the steam condensation rate is proportional to the liquid layer thickness. Also, the steam condensation rate is restricted by the liquid layer thickness. The buoyancy force in a water layer is influenced by the density of water as a function of temperature. The temperature difference between the condensate and the cold-water, which is sub-cooling influence on buoyancy force.

4. CONCLUSIONS

In the present study, experiments for local thermal hydraulic flow characteristics have been performed to obtain the data on the water layer temperature and velocity fields for a co-current steam-water stratified flow in a horizontal rectangular channel. Several advanced measurement methods have been applied to measure local characteristics of the water layer thickness, temperature and velocity fields in a horizontal stratified flow. The instantaneous velocity and temperature fields in the water layer were simultaneously measured using laser induced fluorescence (LIF) and particle image velocimetry (PIV), respectively.

The effects of steam flow velocity on the water layer characteristics were examined for a fixed superficial liquid velocity and inlet layer thickness. The condensation induced flow propagation was investigated. Simultaneous observations of the temperature and velocity distribution enabled us to understand clearly how a condensate is propagate into the lower region of the water layer, leading to the turbulent thermal mixing. Based on the present observations and phenomenological understandings, basic strategy for the analysis was proposed for the interface configuration and turbulent thermal mixing mechanism.

The main conclusions obtained in the present work can be summarized as follows.

(1) The measurements of the temperature and velocity distribution under co-current steam-water stratified flow conditions showed that the condensate is more effectively propagated into the lower region of the water layer when the steam flow velocity increased.
(2) The present heat transfer coefficient is considerably higher than the values calculated by existing correlations of Lim et al. (1984) and Kim and Bankoff (1983). The main reason for this discrepancy can be attributable to the differences in flow direction and the water layer thickness.
(3) The mechanism of the turbulent thermal mixing in a condensing flow is proposed on the basis of kinetic and potential energy exchange. Growth of turbulent thermal mixing depth is explained by implementing turbulent energy budget examination.

NOMENCLATURE

j_k	superficial velocity of phase k (m/s)
T	temperature (°C)
V	velocity (m/s)
u	axial velocity component (m/s)
v	vertical velocity component (m/s)
x	axial distance from the water inlet (m)
y	vertical distance from the bottom wall (m)

Greek symbols

δ_k	thickness of phase k (m)

Subscripts

f	water
g	steam
in	inlet

ACKNOWLEDGMENTS

This work was supported by the National Research Foundation of Korea grant (NRF- 2012M2A8A4004176) funded by Ministry of Science, ICT and Future Planning (MSIP) of the Korean government.

REFERENCES

1. Segev, A., Flanigan, L. J., Kurth, R. E., Collier, R. P., "Experimental Study of Countercurrent Steam Condensation," *J. Heat Transfer*, **103**, pp. 307-311 (1981).
2. Lim, I. S., Tankin, R. S., Yuen, M. C., "Condensation Measurement of Horizontal Cocurrent Steam/Water Flow," *J. Heat Transfer*, **106**, pp. 425-432 (1984).
3. Kim, H. J., Lee, S. C., Bankoff, S. G., "Heat Transfer and Interfacial Drag in Countercurrent Steam-Water Stratified Flow," *Int. J. Multiphase Flow*, **11**, pp. 593-606 (1985).
4. Chu, I.-C., Yu, S. O., Chun, M.-H., Chung, M. K., "Interfacial Condensation Heat Transfer for Countercurrent Steam-Water Stratified Flow in a Circular Pipe," *J. Korean Nuclear Society*, **32**, pp. 142-156 (2000).
5. K.W. Lee, I.C. Chu, S.O. Yu, H.C. No., "Interfacial condensation for countercurrent steam-water stratified wavy flow in a horizontal circular pipe," *Int. J. Heat Mass Transfer*, **49**, pp. 3121–3129 (2006).
6. H.S. Park, S.W. Choi, H.C. No., "Direct-contact condensation of pure steam on co-current and counter-current stratified liquid flow in a circular pipe," *Int. J. Heat Mass Transfer*, **52**, pp. 1112–1122 (2009).